

ELEMENTS OF LASER SYSTEMS

PACS numbers: 42.55.Rz; 42.60.By; 42.79.Bh; 42.79.Ci
DOI: 10.1070/QE2013v043n11ABEH015288

Short spatial filters with spherical lenses for high-power pulsed lasers

K.F. Burdonov, A.A. Soloviev, A.S. Egorov, A.A. Shaikin, A.K. Potemkin

Abstract. **We report possible employment of short spatial filters based on spherical lenses in a pulsed laser source (neodymium glass, 300 J, 1 ns). The influence of the spherical aberration on the quality of output radiation and coefficient of conversion to the second harmonics is studied. The ultra-short aberration spatial filter of length 1.9 m with an aperture of 122 mm is experimentally tested. A considerable shortening of multi-cascade pump lasers for modern petawatt laser systems is demonstrated by the employment of short spatial filters without expensive aspherical optics.**

Keywords: *petawatt laser, neodymium glass pump laser, spatial radiation quality, spatial filter.*

1. Introduction

The energy of laser radiation at output of modern petawatt OPCPA systems [1–5] is actually determined by the pump parameters of final power parametric amplifying stages. The pump laser pulse [6, 7] in addition to a sufficient energy should also have highly uniform spatial distributions of phase and amplitude and a uniform time profile.

Spatial filters (SFs) [8] in the pump lasers for OPCPA systems, in addition to filtration of a high-frequency component of the spatial spectrum, also perform beam scaling in the process of amplification to reduce nonlinear effects, and transfer radiation between active elements. The absence of filtration results in a breakdown of the active elements and transporting mirrors due to the beam self-focusing [9, 10].

High requirements to phase aberrations impose substantial limitations on the minimal length of the SF. For example, for a beam with an aperture of 120 mm the minimal length of an aberration-free SF with spherical lenses is ~4 m. Telescope shortening due to the employment of lenses with a shorter focal length increases aberrations, first of all, the spherical one, which negatively affects the efficiency of conversion to the second harmonic.

K.F. Burdonov, A.A. Soloviev Institute of Applied Physics, Russian Academy of Sciences, ul. Ul'yanova 46, 603950 Nizhnii Novgorod, Russia; N.I. Lobachevsky State University of Nizhnii Novgorod, ul. Minina 24, 603600 Nizhnii Novgorod, Russia; e-mail: kfb.iap@gmail.com;
A.S. Egorov N.I. Lobachevsky State University of Nizhnii Novgorod, ul. Minina 24, 603600 Nizhnii Novgorod, Russia;
A.A. Shaikin, A.K. Potemkin Institute of Applied Physics, Russian Academy of Sciences, ul. Ul'yanova 46, 603950 Nizhnii Novgorod, Russia

Received 19 July 2013; revision received 28 August 2013
Kvantovaya Elektronika **43** (11) 1082–1087 (2013)
Translated by N.A. Raspopov

Since there may be sufficiently many filters per channel, at the radiation beam aperture of above 100 mm they actually determine the dimensions of the entire laser installation. The employment of aspheric elements is hindered by a noticeably higher price of creating and servicing the laser system. Hence, the problem of determining the minimal admissible length of the SF with spherical lenses at high quality of the phase front and efficiency of conversion to the second harmonic seems principally important.

In the present work, the extremely short aberration-free SF of length 2 m is tested in the system for pumping a power cascade of the PEARL petawatt laser complex [4]. Such characteristics as the transmission coefficient, temporal profile of laser pulse (pulse 'cleavage'), coefficient of the following conversion of radiation to the second harmonic, and spatial quality of pulse at the frequency of the second harmonic were studied.

2. Spherical aberration in SF with spherical lenses

In high-power pulsed lasers the radiation is usually transported between active elements by using SFs. A spatial filter is a confocal Kepler telescope comprising two coaxial collecting lenses L1 and L2 with the focal lengths f_1 and f_2. In the construction of the PEARL installation, the lenses are windows of a metal vacuum cell (Fig. 1). Such an optical system transfers an image with magnification $M = f_2/f_1$ from plane P1 to plane P3, in which active elements are usually placed; the distances l_1 and l_2 are related by the relationship $l_2 = M(f_1 + f_2 - Ml_1)$. To avoid an optical breakdown, the space around the beam waist between the lenses is evacuated. In the waist plane P2, the diaphragm is placed which performs the spatial filtration (blocks high-frequency components in the spatial spectrum).

In the present work, the SF is investigated at the radius of input beam $h_0^{\text{in}} = 47$ mm and radius of output beam $h_0^{\text{out}} = 61$ mm. The centre wavelength of laser radiation is $\lambda = 1054$ nm.

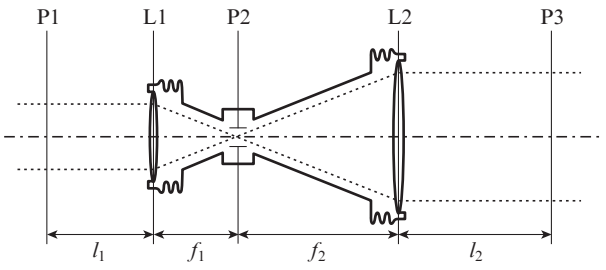

Figure 1. Schematic diagram of the SF.

The pressure inside the filter was maintained at the level of 10^{-3} Torr. For convenience of adjusting the filtering diaphragm was motorised.

The problem of keeping the plane wave front of the laser beam, that is, its diffraction quality, imposes limitations on the minimal length of the SF with spherical lenses.

By analogy to Marechal's criterion [11] we will call the radiation aberration-free if the rms distortions of its phase front do not exceed 1/14 of the wavelength:

$$D(W) < \lambda/14, \tag{1}$$

which, for small aberrations W, corresponds to a Strehl ratio St > 0.8 [12]. For the spherical aberration, Marechal's criterion well agrees with the Rayleigh criterion for the peak phase distortion value

$$\mathrm{PV}(W) < \lambda/4. \tag{2}$$

In the case of monochromatic radiation, the aberrations of thin spherical lenses are mainly related with spherical aberrations. The spherical aberration of a collecting lens is revealed in the deflection of peripheral rays from the ideal trajectory by an angle α_s (Fig. 2). This results in the shift of the converging point by a distance x_s and blurring of the point image to a circle of scattering with a radius r_s. Parameters α_s, x_s and r_s are termed angular, longitudinal and transversal spherical aberrations, respectively:

$$x_s = Uh_0^2/\mathrm{f},\ r_s = Uh_0^3/f^2,\ \alpha_s = Uh_0^3/f^3, \tag{3}$$

where f is the focal distance of lens; h_0 is the beam radius; and U is Seidel's parameter dependent on the radii of curvature of lens surfaces $R_{1,2}$ and on the refractive index n [12].

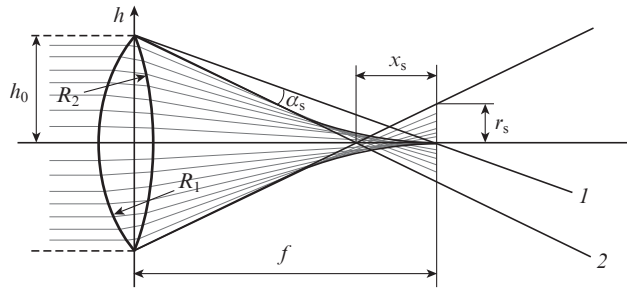

Figure 2. Ray paths in a diffraction-free thin lens: peripheral ray trajectory in the case (*1*) without spherical aberration and (*2*) with the aberration.

For the spherical lens made of a material with $n = 1.5$, spherical aberrations are minimal at the ratio of radii $R_2/R_1 = -1/6$.

In considering the telescope, the aberration lens may be presented as two successive elements: an aberration-free lens and the aberration plate which introduces phase aberrations $w(r) = \int \alpha(r)\,\mathrm{d}r$, where α is the angular aberration. The total phase aberrations of the confocal telescope $W(r)$ comprise the aberrations of its lenses making the allowance for scaling factor M:

$$W(r) = \frac{1}{M} w_1\left(\frac{r}{M}\right) + w_2(r), \tag{4}$$

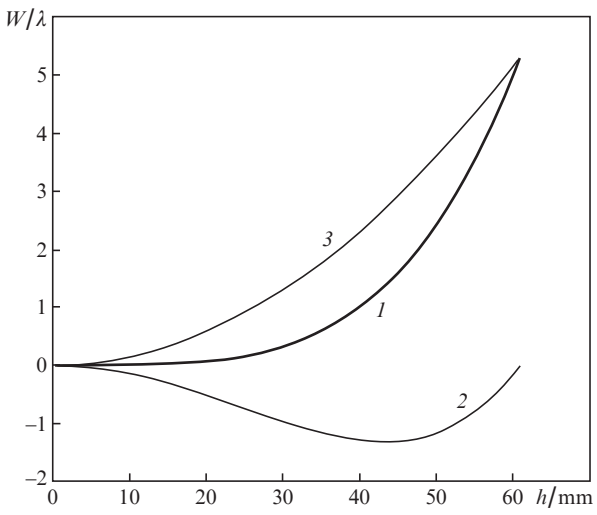

Figure 3. Wavefront distortions for the beam of radius $h_0^{\mathrm{out}} = 61$ mm at the output of the telescope of length 1.9 m with the magnification $M = 1.3$: (*1*) total aberrations of the spherical lens W, (*2*) spherical aberration W_{sph} and (*3*) defocusing W_{def}. For convenience of comparison the dependences are plotted starting from zero.

The value of $W(r)$ formally is the sum of two radial Zernike polynomials: defocusing $W_{\mathrm{def}} = C_{02}[2(r/h)^2 - 1]$ and spherical third-order aberration $W_{\mathrm{sph}} = C_{04}[6(r/h)^4 - 6(r/h)^2 + 1]$, where C_{02} and C_{04} are amplitude coefficients (Fig. 3).

One can easily show that in the case of only spherical aberration W_{sph} it follows from Rayleigh criterion (2) that

$$\mathrm{D}(W_{\mathrm{sph}}) < \sqrt{5}\lambda/30, \tag{5a}$$

$$\mathrm{PV}(W_{\mathrm{sph}}) < 2\lambda/h_0. \tag{5b}$$

Note that inequality (5a) is close to Marechal's criterion (1), and inequality (5b) means that a maximal angle between the normal to the wavefront surface and the axis of the system is approximately twice the angular dimension of first minimum of the far-field intensity distribution for the radiation beam of radius h_0 with plane wave- and amplitude fronts:

$$A_{\mathrm{dif}} = 2.44\lambda/(2h_0). \tag{6}$$

Dependences of the peak and rms values of spherical aberration on the telescope length $L = f_1 + f_2$ with the magnification $M = 1.3$ at the input beam radius $h_0^{\mathrm{in}} = 47$ mm and $n = 1.508$ are shown in Fig. 4. The horisontal lines mark the levels $W = \lambda/14$ and $\lambda/4$. One can see that the spherical aberration introduced by the filter is immaterial at the telescope length $L > 3.2$ m.

Another criterion for the value of radiation aberration is the coefficient of conversion to the second harmonic. Under matched synchronism (for example, when the refractive index for an ordinary wave at the resonance frequency is equal to that of an extraordinary wave at the frequency of second harmonic) the maximal conversion coefficient in the crystal may reach unity. However, the spherical aberration breaks exact spatial matching of synchronism over the whole beam aperture simultaneously, and the integral conversion coefficient falls. The local conversion coefficient η near the matched angle depends on the detuning $\Delta\theta$ [13]:

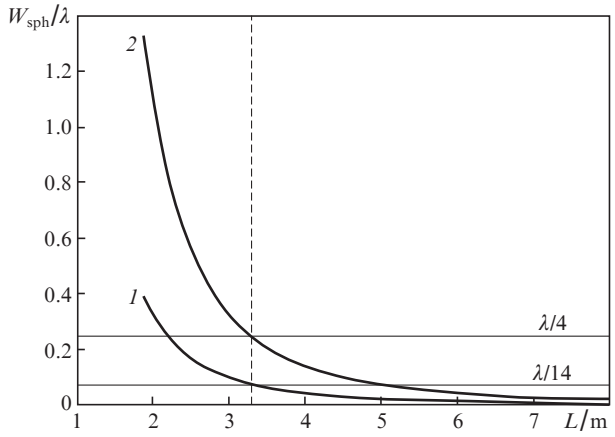

Figure 4. Spherical aberration vs. the length of the telescope with $M = 1.3$ at $h_0^{in} = 47$ mm: (*1*) the rms value of spherical aberration and (*2*) amplitude of spherical aberration; the vertical dashed line denotes the limit of telescope aberration-free operation.

$$\eta = \frac{\sin^2(B\Delta\theta)}{(B\Delta\theta)^2}, \qquad (7)$$

where $B = \pi/(9.5\times10^{-4})$. For the KD*P crystal employed the coefficient B was experimentally found by the detuning angles for first minima. The detuning $\Delta\theta$, in turn, is related to the angular aberration α by the relationship $\Delta\theta = \alpha\sin\varphi$, where φ is the polar angle. By integrating (7) over the beam aperture we obtain the dependence of the integral coefficient of conversion to the second harmonic on the telescope length, which is presented in Fig. 5. One can see that at the SF length of less than 1.25 m, the limiting value of the integral coefficient of conversion to the second harmonic reduces by more than 10%. This length can be considered ultimately short for the telescope with $h_0^{in} = 47$ mm and $h_0^{out} = 61$ mm. Nevertheless, after the telescope of length 1.9 m under consideration, the integral coefficient of conversion to the second harmonics reduces by less than 1%.

Note that if several filters are used in the scheme, then the estimates given above should be made for the summed aberrations and the minimal admissible lengths of separate filters would increase.

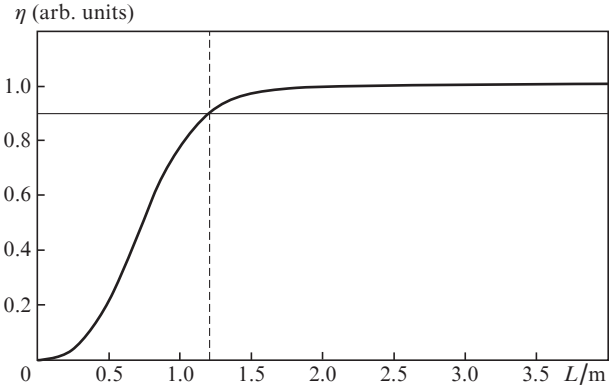

Figure 5. Estimated maximal achievable efficiency of conversion to the second harmonic vs. the length of the SF with spherical lenses at the radius of input radiation beam $h_0^{in} = 47$ mm and output beam $h_0^{out} = 61$ mm.

3. Experiments

3.1. Scheme of the experiment

The third stage of the parametric amplifier in the PEARL OPCPA installation [4] is pumped by pulsed radiation of duration 1 ns at the beam aperture of 122 mm at the second harmonic frequency of the neodymium laser, thus, adding to the energy of signal radiation the value of ~30 J. In tests, the short SF was placed in the pump laser according to the schematic diagram shown in Fig. 6.

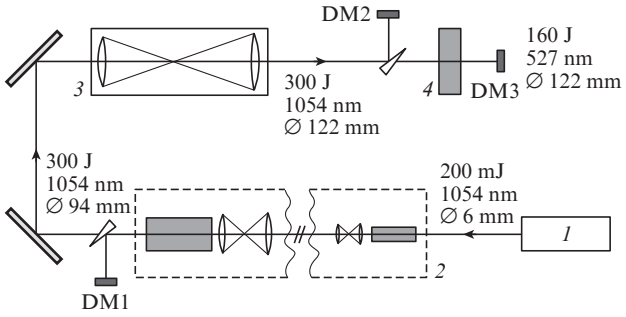

Figure 6. Principal optical scheme of the experimental setup: (*1*) driving Nd:YLF generator; (*2*) multistage laser amplifier; (*3*) SF under study; (*4*) nonlinear KD*P crystal; DM1 and DM2 are radiation diagnostic modules.

The driving Nd:YLF-laser (*1*) provides the pulses of duration 1 ns with the energy of 180 mJ at the wavelength of 1054 nm [6]. After the driving generator, the radiation passes to the multistage amplifier (*2*), which comprises the system forming the spatial beam structure [14], and to seven successive active elements made of phosphate neodymium glass with the SFs placed between them, which provide a diffraction-quality beam. The pumping of active elements is made by pulsed flash-lamps. The amplifier operates in the regime of one shot per 15 min. The pulse repetition rate is limited by thermal effects in the active elements. At the output from the last active element of the amplifier the laser pulse with the beam cross-section diameter of 94 mm has the energy of ~300 J (Fig. 7).

The investigated object is the output SF (*3*) of the multistage amplifier, which increases the cross-section diameter of laser radiation beam to 122 mm. After amplification the laser

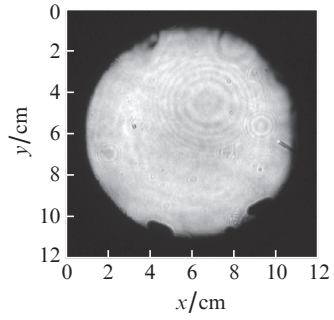

Figure 7. Cross-section intensity distribution at the amplifier output and the pulse energy of 300 J. Imperfections at the beam periphery are caused by cleaved faces of neodymium glass active elements.

Table 1. Characteristics of SFs under study.

SF	L/mm	M	Input lens			Output lens			Diameter of diaphragm/mm
			R_1/mm	R_2/mm	f_1/mm	R_1/mm	R_2/mm	f_2/mm	
Diffraction	9103	1.28	2208	–24210	3991	2884	–25590	5112	3
Short	1877	1.27	461	–4529	826	597	–4966	1051	1.4

pulse passes to the nonlinear KD*P crystal (*4*), in which the radiation is converted to the second harmonic. The quality of the laser beam is controlled by a diagnostic system arranged before and after the output SF and also after the DK*P crystal (diagnostic modules DM1–DM3). Module DM1 comprises a pyrometric energy meter, the diode for detecting the time profile of the pulse, and a CCD-array for measuring the spatial distribution of the radiation intensity and its depolarised component. Module DM3 includes the pyrometric energy meter, two CCD-arrays for measuring the spatial intensity distributions of fundamental and second-harmonic radiation, and the diode for detecting the doubled component. The additional diagnostic module DM2, which is absent under normal laser operation, comprises the wavefront sensor and the CCD-array for measuring the spatial distribution of the aberration amplitude.

Under normal operation of the PEARL system, the aberration-free filter of length ~9 m is placed instead of the SF (*3*). In Table 1, the parameters of the standard and investigated PFs are presented.

The size of the diaphragm hole was tested experimentally. The size was proper if it provided the required degree of spatial filtration while keeping the filter transmission at the energy of ~300 J. For diffraction-quality filtration, the diaphragm was used with the diameter of about 30 times greater than the characteristic waist dimension $A_{\text{dif}}f_1$. For the short aberration filter, the latter ratio was enlarged to 70 to avoid diaphragm 'blackout' due to its ionisation by wings of focal intensity distribution [15, 16].

According to [6, 8], for the intensity $I = 4$ GW cm^{-2} realised in our experiments, the typical angular dimension of phase irregularities in a phosphate glass due to small-scale self-focusing was 2×10^{-3} rad. The ratio of the diaphragm radius to focal distance of input lens in the filter under investigation was 0.85×10^{-3}, which provided efficient suppression of small-scale self-focusing.

3.2. Influence of spherical aberration on the output parameters of pump laser radiation

The presence of the spherical aberration in radiation introduced by the short SF may reduce the energy and worsen the spatial and temporal distributions of the pump pulse intensity.

There are several mechanisms for the worsening. First, the aberrations lead to energy redistribution from the Airy disk to the wings of focal intensity distribution, which may interact with the filtering diaphragm. This may cause ionisation of diaphragm material and, as a consequence, 'cleave' the pulse rare edge, distort the cross-section amplitude distribution, and reduce the transmission coefficient. Such effects can hardly be estimated and numerically modelled; this is why the optimal size of the diaphragm was determined experimentally. Similar effects may be observed due to a breakdown in the vicinity of beam waist even without ionisation of diaphragm. Hence, vacuum in the SF should be thoroughly controlled.

Second, the process of second harmonic generation is rather sensitive to spherical aberrations. In the case of a wide spatial spectrum the phase matching between the radiation of fundamental and second harmonic waves is not fulfilled for all angular components. This results in the nonuniform coefficient of conversion to the second harmonic over the beam aperture and reduces its integral value. The conversion efficiency η depends on the intensity and it is also important to control the uniformity of the near-field intensity distribution at the fundamental frequency.

Thus, in using a short SF it is necessary to control the following characteristics: the transmission coefficient of the filtering diaphragm at low and high energies, time profile of the pulse, amplitude distribution and shape of the phase front of beam, and air pressure in the filter.

3.2.1. Transmission of filters and time 'cleavage' of the pulse

Radiation energy losses in SFs are related with reflection losses on lens surfaces and with pulse 'cleavage' due to plasma formation in the vicinity of the beam waist. In the short SF and standard diffraction-quality SF the losses were 7% in the energy range 0–300 J.

Oscillograms of laser radiation pulses at the input and output of long and short SFs measured by a Thorlabs SV2-FC photodiode and Agilent 54835 Infinium oscilloscope are presented in Fig. 8. The instrument function width of the photodiode–oscilloscope system was ~0.1 ns. One can see that the pulse shape and duration do not change while passing both through the diffraction-quality SF and through the short SF. This means that at the radiation energy close to 300 J and diaphragm diameters given in Table 1, 'cleavage' of the pulse by plasma in the vicinity of filtering diaphragm is not observed.

3.2.2. Phase front of radiation

The phase front of laser radiation was controlled by a DVF-200 Shack–Hartmann sensor. In Table 2, the total amplitudes of spherical aberration are given for the SF under study and for the aberration-free telescope. One can see that the aberrations of the standard SF are beyond the measurement accuracy. The aberrations of the short filter are noticeable and well agree with the calculations [see Fig. 4 and formula (5)]. The accuracy of measurements of the total amplitude of spherical aberration by the wavefront sensor is $\lambda/10$ (~100 nm). The aberrations measured are independent of the energy of laser radiation, which testifies that ionisation in the vicinity of the beam waist in the SF is negligible.

Table 2. Values of spherical aberrations for filters under study, measured by the wavefront sensor.

SF	Energy/J	Total amplitude of spherical aberrations/λ	Root mean square deviation of spherical aberrations/λ
Aberration-free	100–300	0	0
Aberration	100–300	1.5	0.5

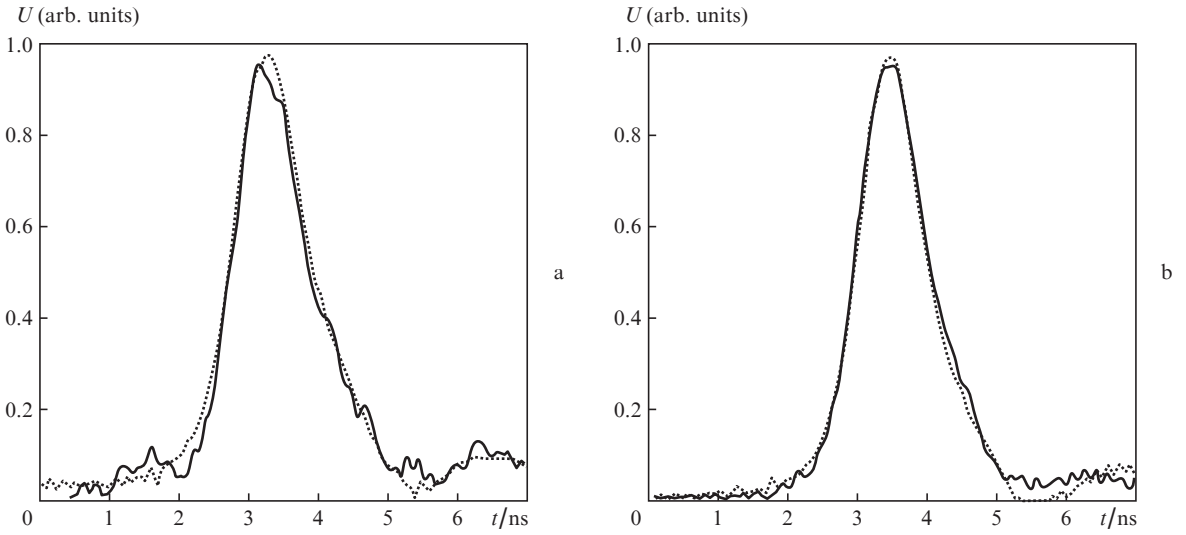

Figure 8. Oscillograms of radiation pulses at (dashed) the input and (solid) output of (a) the aberration-free SF of length 9.1 m and of (b) the short SF of length 1.9 m at the pulse energy of 280 J.

3.2.3. Second harmonic generation

The main experiment capable of revealing the possibility of using a short SF in the pump laser is generation of the second harmonic. Images of the cross-section intensity distribution for the second harmonic of laser radiation with employed SFs are shown in Fig. 9. In both the cases, at the energy of fundamental-frequency radiation 280 J, the energy of the second harmonic was 182 J. The technical efficiency of conversion to the second harmonic is 57%, and the physical efficiency (that is, without losses in the KD*P crystal and on its faces) is 65%.

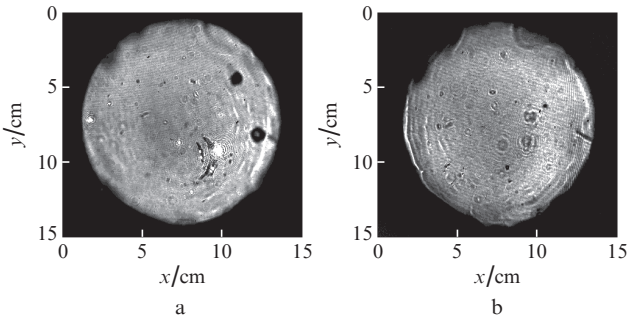

Figure 9. Cross-section distributions of the radiation intensity at the frequency of the second harmonic for (a) the diffraction-quality SF and (b) for the short SF.

The technical efficiency of the second harmonic generation is shown in Fig. 10 versus the energy of radiation passing to the KD*P crystal. The accuracy of energy measurements is 7%. The short aberration SF introduced into the scheme neither worsened noticeably the quality of the second harmonic in the near-field zone, nor reduced the conversion efficiency.

4. Conclusions

A short aberration SF was investigated for the laser pump system (1054 nm, neodymium glass, 300 J, 1 ns) of the PEARL petawatt complex.

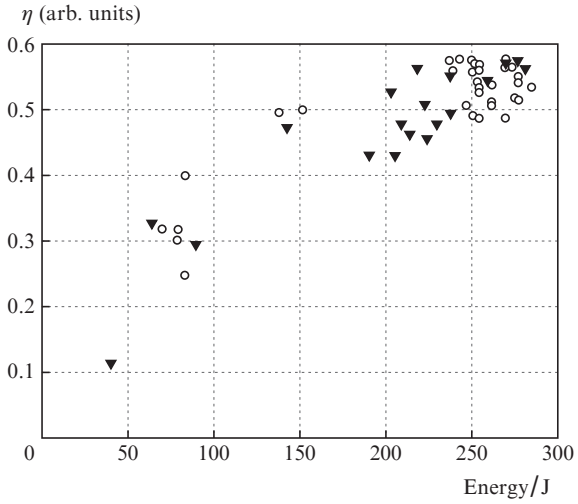

Figure 10. Efficiency of output radiation conversion to the second harmonic in the KD*P crystal of length 25.5 mm while using (○) the diffraction-quality SF and (▼) short SF.

In the theoretical part, the expressions are presented for estimating the spherical aberration introduced by the spherical lenses comprised in the filter. The minimal length is calculated for the telescope spherical lenses, which satisfies Marechal's criterion for wave aberrations.

In the theoretical part of the work, the short (length of 1.9 m, output aperture of 130 mm) filter was tested in the pump laser of a final parametric stage of the PEARL complex. The influence of introduced spherical aberrations on the transmission coefficient, on phase distribution of radiation at output of SF, and on efficiency of conversion to the second harmonic was studied. Keeping in mind the effects related to ionisation of the diaphragm, the tests were performed at energies close to the calculated value (300 J). It was shown that despite the spherical aberration introduced by the filter, which reached 1.5λ in amplitude, the amplitude distribution of the radiation pulse after frequency doubling and the efficiency of conversion to the second harmonic remained the same as with the long filter.

Thus, the possibility of substantial shortening of multi-stage pump lasers of modern lasers of petawatt power by employing short SFs without expensive aspherical optics has been demonstrated.

Acknowledgements. The work was partially supported by the Ministry of Education and Science of the Russian Federation (Contract Nos 11.G34.31.0011 and 14.518.11.7071).

References

1. Ross I.N. et al. *Opt. Commun.*, **144**, 9 (1997).
2. Lozhkarev V.V. et al. *Pis'ma Zh. Eksp. Teor. Fiz*., **82** (4), 196 (2005).
3. Lozhkarev V.V. et al. *Opt. Express*, **14**, 9 (2006).
4. Lozhkarev V.V. et al. *Laser Phys. Lett*., **4**, 7 (2007).
5. Soloviev A.A. et al. *Nucl. Instrum. Methods Phys. Res., Sect. A*, **653** (1), 35 (2011).
6. Poteomkin A.K. et al. *Kvantovaya Elektron.*, **35**, 302 (2005) [*Quantum Electron*., **35**, 302 (2005)].
7. Poteomkin A.K. et al. *IEEE J. Quantum Electron.*, **45** (7), 9 (2009).
8. Potemkin A.K. et al. *Appl. Opt.*, **46** (20), 8 (2007).
9. Mustaev K.S. et al. *Pis'ma Zh. Tekhn. Fiz*., **6** (14), 856 (1980).
10. Poteomkin A.K. et al. *IEEE J. Quantum Electron.*, **45** (4), 9 (2009).
11. Marechal A. *Rev. d'Optique*, **26**, 257 (1947).
12. Born M., Wolf E. *Principles of Optics* (Oxford: Pergamon Press, 1969; Moscow: Nauka, 1970).
13. Akhmanov S.A., Nikitin S.Yu. *Fizicheskaya optika* (Physical Optics) (Moscow: Nauka, 2004).
14. Mart'yanov M.A. et al. *Kvantovaya Elektron*., **38**, 354 (2008) [*Quantum Electron*., **38**, 354 (2008)].
15. Murray J.E. et al. *Proc. SPIE Int. Soc. Opt. Eng.*, **3047**, 207 (1998).
16. Bikmatov R.G. et al. *Proc. SPIE Int. Soc. Opt. Eng.*, **3492**, 510 (1999).